Published in final edited form as:
Cancer Res. 2008 September 15; 68(18): 7362–7370. doi:10.1158/0008-5472.CAN-08-0575.

Nordihydroguaiaretic Acid Inhibits an Activated FGFR3 Mutant, and Blocks Downstream Signaling in Multiple Myeloma Cells

April N. Meyer, **Christopher W. McAndrew**, and **Daniel J. Donoghue***
Department of Chemistry and Biochemistry, Moores UCSD Cancer Center, University of California San Diego, La Jolla, California 92093-0367, Tel: 858-534-2463, Fax: 858-534-7481, Email: ddonoghue@ucsd.edu

Abstract

Activating mutations within Fibroblast Growth Factor Receptor 3 (FGFR3), a receptor tyrosine kinase, are responsible for human skeletal dysplasias including achondroplasia and the neonatal lethal syndromes, Thanatophoric Dysplasia (TD) type I and II. Several of these same FGFR3 mutations have also been identified somatically in human cancers, including multiple myeloma, bladder carcinoma and cervical cancer. Based on reports that strongly activated mutants of FGFR3 such as the TDII (K650E) mutant signal preferentially from within the secretory pathway, the inhibitory properties of nordihydroguaiaretic acid (NDGA), which blocks protein transport through the Golgi, were investigated. NDGA was able to inhibit FGFR3 autophosphorylation both *in vitro* and *in vivo*. In addition, signaling molecules downstream of FGFR3 activation such as STAT1, STAT3 and MAPK were inhibited by NDGA treatment. Using HEK293 cells expressing activated FGFR3-TDII, together with several multiple myeloma cell lines expressing activated forms of FGFR3, NDGA generally resulted in a decrease in MAPK activation by 1 hour, and resulted in increased apoptosis over 24 hours. The effects of NDGA on activated FGFR3 derivatives targeted either to the plasma membrane or the cytoplasm were also examined. These results suggest that inhibitory small molecules such as NDGA that target a specific subcellular compartment may be beneficial in the inhibition of activated receptors such as FGFR3 that signal from the same compartment.

Keywords

FGFR; NDGA; multiple myeloma; bladder carcinoma; TDII

Introduction

Receptor tyrosine kinases (RTKs) represent important signal transducers for the transmission of information across the cell membrane, including 58 distinct receptors in 16 different families of homologous proteins in humans (1,2). The Fibroblast Growth Factor Receptor (FGFR) family includes four closely related receptors, designated FGFR1, FGFR2, FGFR3 and FGFR4. All FGFRs exhibit a cleaved N-terminal signal sequence that directs the nascent protein into the endoplasmic reticulum (ER), followed by three extracellular immunoglobulin (Ig)-like domains, a membrane-spanning domain and a split tyrosine kinase domain (3,4), and are activated by Fibroblast Growth Factors (FGFs), a large family of some 20 related growth factors (5–8). The ligand-binding specificity differs for each FGFR family member, with alternative splicing of FGFR transcripts resulting in further distinctions in ligand specificity accompanied by altered biological properties (4,9). FGFR activation controls an array of

*To whom correspondence should be addressed. E-mail: ddonoghue@ucsd.edu.

biological processes, including cell growth, differentiation, migration, wound healing and angiogenesis. Aberrant activation of these receptors, often through gain-of-function mutations, is associated with many developmental and skeletal disorders. Mutational activation of FGFR3 is responsible for the relatively common skeletal dwarfism, achondroplasia, due to the G380R mutation within the transmembrane domain, whereas strong activation by the mutation K650E within the kinase domain results in the neonatal lethal syndrome, Thanatophoric Dyspasia Type II (TDII) (10).

Aberrant signal transduction arising from expression of a constitutively activated FGFR3 is also an important event in a variety of human neoplasias, especially multiple myeloma and bladder carcinoma (11–15). Multiple myeloma is typified by the accumulation of secretory plasma cells in the bone marrow, which exhibit low proliferation but an extended life span. A frequent translocation observed in multiple myeloma, t(4;14)(p16.3;q32.3), involves the FGFR3 gene, and results in increased expression of FGFR3 alleles (11,12). This translocation occurs with an incidence of about 20% in multiple myeloma, and places the FGFR3 gene located at 4p16.3 in proximity with the 3′ IgH enhancer at 14q32.3, leading to significant FGFR3 overexpression (11). Furthermore, FGFR3 overexpression is often accompanied by mutational activation, including the mutations Y373C and K650E, corresponding to germline FGFR3 mutations that cause the lethal skeletal syndromes TDI and TDII, respectively (10, 16). The aberrant signaling of overexpressed, mutated FGFR3, acting in concert with other dysregulated genes such as cyclin D1, c-maf, and MMSET, evidently contributes to the increased proliferative potential of B-cell myelomas (17). Mutational activation of FGFR3 has also been reported in human bladder and cervical carcinomas (13–15), including the mutations corresponding to R248C, S249C, G370C and K650E, previously identified as causing TDI or TDII (10,16).

Several recent reports demonstrate that the high level of kinase activity associated with the strongly activated FGFR3 mutants such as TDII (K650E) leads to accumulation of immature/mannose-rich, phosphorylated receptors in the ER. This can result in direct recruitment of Jak1 and activation of STAT1 from the ER, as well as activation of Erk1/2 from the ER through a FRS2-independent and PLCγ-independent pathway (18–20). Given the ability of FGFR3 to signal from intracellular compartments within the secretory pathway, we investigated the possible inhibitory properties of a drug that specifically blocks ER/Golgi transport. Nordihydroguaiaretic acid (NDGA), a naturally occurring polyhydroxyphenolic compound isolated from the creosote bush, *Larrea divaricatta*, has been previously characterized as a lipoxygenase inhibitor, as a strong antioxidant, and as an inhibitor of protein transport from the ER to Golgi, leading to a redistribution of Golgi proteins to the ER (21–24). NDGA has also been shown to have effects on cell proliferation, apoptosis and differentiation. Recently, it was shown to have potentially valuable inhibitory effects against specific receptor tyrosine kinases (RTKs) such as IGF-1R, HER2/neu and PDGFR (25–28).

The experiments presented here explore the ability of NDGA to inhibit signaling by activated FGFR3, including kinase activation and downstream signaling associated with an activated receptor. Given the ability of NDGA to inhibit other RTKs, and the ability of NDGA to collapse the secretory compartment from which activated FGFR3 is known to signal (18–20), we examined the possibility that NDGA would be particularly effective against the strongly activated FGFR3 mutant K650E. Indeed, NDGA was able to inhibit activation of the downstream signaling proteins STAT1, STAT3 and MAPK. In addition, NDGA increased apoptosis in cells expressing FGFR3-TDII, as measured by PARP cleavage. NDGA was also able to increase apoptosis in the multiple myeloma cell line KMS-18 that expresses high levels of FGFR3 G384D. To examine possible therapeutic effects of NDGA, multiple myeloma-derived cell lines were treated with FGF2 to activate FGFR3, and the effects of NDGA treatment on downstream signaling pathways were observed. The results are discussed with

respect to other therapeutic approaches for treatment of cancers presenting overexpressed and/or mutated FGFR3.

Materials and Methods

FGFR Constructs

The full-length wild-type and kinase active (TDII:K650E) FGFR3 have been described previously (29). The membrane-localized kinase domain derivatives of FGFR3 have also been previously described (30).

Antibodies and Reagents

Antibodies were obtained from the following sources: FGFR3 (C-15), STAT1 (E-23), STAT3 (C-20), β-tubulin (H-235) - Santa Cruz Biotechnology; 4G10 (anti-phosphotyrosine) - Upstate Biotechnology; Phospho-STAT1 (Tyr701), Phospho-STAT3 (Tyr705) (D3A7), Phospho-p44/42 MAPK (Thr202/Tyr204) (E-10), cleaved PARP (Asp214) – Cell Signaling; MAP Kinase (ERK1 + ERK2) – Zymed; HRP anti-mouse and HRP antirabbit - Amersham. mAb 10E6 was a gift from V. Malhotra Lab, UCSD. Fluorescein-conjugated anti-mouse (Sigma). Rhodamine-conjugated anti-rabbit (Boehringer-Mannheim). NDGA and the poly (4:1 Glu, Tyr) peptide were obtained from Sigma. Zilueton was a gift from Dr. Edward Dennis, UCSD.

Immunoprecipitation and Immunoblot

HEK293 cells were grown in Dulbecco's Modified Eagle's Medium (DMEM), supplemented with 10% fetal bovine serum (FBS) and incubated at 37°C in 10% CO_2. 9×10^5 cells plated on 10cm dishes were transfected the next day with 2μg of DNA by calcium phosphate precipitation at 3% CO_2, as previously described (31,32). After 18–20h cultures were moved back into 10% CO_2 for 4–6h before starving in 0% DMEM or treating with NDGA in 10% FBS DMEM overnight. Cultures that were starved overnight were treated with NDGA at varying concentrations or time, as indicated in Figure Legends. Cells were harvested, washed once in PBS and lysed in 1% NP-40 Lysis Buffer [20mM Tris-HCl (pH 7.5), 137mM NaCl, 1% Nonidet P-40, 5mM EDTA, 50mM NaF, 1mM sodium orthovanadate, 1mM phenylmethylsulfonyl fluoride (PMSF), 10μg/mL aprotinin] or RIPA Lysis Buffer [50mM Tris-HCl (pH 8.0), 150mM NaCl, 1% Nonidet P-40, 0.5% DOC, 0.1% SDS, 50mM NaF, 1mM sodium orthovanadate, 1mM phenylmethylsulfonyl fluoride (PMSF), 10μg/mL aprotinin]. Total protein was measured by Bradford Assay or Lowry Assay. Lysates were immunoprecipitated with antibody for 2h at 4°C. Protein A-Sepharose beads were added and incubated for 2 h at 4°C. The immunoprecipitated samples were washed 3 times with Lysis Buffer, boiled 5 min in sample buffer, and separated by 10% SDS-PAGE. Proteins were transferred to Immobilon-P membranes (Millipore) and blocked in 3% milk/TBS/0.05% Tween-20 or 3%BSA/TBS/0.05% Tween-20 (for anti-phosphotyrosine, anti-phospho-STAT1 and anti-phospho-STAT3 blots). Membranes were immunoblotted with antibodies at RT for 2 h or overnight at 4°C. After primary incubation, membranes were washed with TBS/0.05% Tween-20 and incubated with HRP conjugated secondary antibodies. Proteins were detected by enhanced chemiluminescence (ECL) (Amersham) or (Millipore). To reprobe with other antibodies, membranes were stripped of bound antibodies in stripping buffer [100 mM 2-mercaptoethanol, 2% SDS, 62.5mM Tris-HCl (pH 6.8)] and incubated for 1 h at 55°C.

In vitro kinase assays

FGFR3-TDII was immunoprecipitated from 500μg of total cell lysate per sample for 1.5 h at 4°C. Protein A-sepharose beads were added for 2 h. After 3 washes with Lysis Buffer samples were washed 1 time with Kinase Buffer [20mM Tris pH 7.5, 10mM $MnCl_2$, 5mM $MgCl_2$]. Immunoprecipitates were preincubated with NDGA in Kinase Buffer for 15 min on ice before

the addition of ATP and the poly (4:1 Glu, Tyr) peptide and incubated at 37°C for 15–25 min. Reactions were washed 3 times with cold Lysis Buffer before adding sample buffer. Proteins were separated by 7.5% or 10% SDS-PAGE and transferred to Immobilon-P membranes for immunoblotting, except for ^{32}P-labeled samples in which the gels were dried and exposed to film or a phosphor screen for use with a Phosphorimager.

Double label indirect immunofluoresence

HEK293 cells were seeded onto Collagen type I coated glass coverslips (BD Biosciences) and transfected as above. After starving overnight cells were treated with 30μM NDGA. At indicated time points coverslips were fixed with 3% paraformaldehyde/PBS for 15 min., washed with PBS and placed at −20°C in 50% glycerol/PBS. Prior to staining, cells were washed with PBS, permeabilized with 0.5% Triton X-100/PBS and blocked with 3% BSA/PBS. The cis-Golgi was detected with monoclonal AB 10E6 and fluorescein-conjugated anti mouse secondary antibody. FGFR3 localization was detected with rabbit polyclonal antibody FGFR3 (C-15) and rhodamine-conjugated anti rabbit secondary antibody. The nuclei were visualized by Hoechst dye added to the Rh secondary antibody mix. All antibodies were diluted in 3% BSA/PBS and incubations performed at room temperature. Coverslips were mounted on glass slides with 90% glycerol in 0.1M Tris (pH 8.5) plus phenylenediamine and photographed using a Nikon Microphot-FXA with a cooled CCD camera (Hamamatsu C5810).

Multiple Myeloma cell lines

The human multiple myeloma cell lines, RPMI-8226, LP-1, KMS-18 and KMS-11, were a generous gift from Dr. Leslie Thompson, UCI. They were grown in RPMI 1640 with L-glutamine media, supplemented with 10% FBS and pen/strep and incubated at 37°C in 5% CO_2. For FGF stimulation, 3×10^6 cells per 35mm well were starved overnight in serum-free RPMI 1640. NDGA was added to the cultures for 1 h at 37°C before simulating with 10ng/ml FGF2 and 1 μg/ml Heparin for 10min. at 37°C. Plates were put on ice and cells were collected, transferred to tubes and spun down for 2 min at 1krpm. Cell pellets were washed once with PBS prior to the addition of RIPA Lysis Buffer. 30 μg of total lysate was separated by 10% SDS-PAGE and processed for immunoblotting as described above. For NDGA treatment of the KMS-18 and KMS-11 cell lines, 6×10^6 cells per 5cm plate were incubated at 37°C with various concentrations of NDGA for 1 h or overnight. Cells were collected by centrifugation as described above. 30 μg of total lysate was separated by 10% SDS-PAGE and transferred to Immobilon-P membranes for immunoblotting.

Results

In vitro inhibition of FGFR3-TDII autophosphorylation by NDGA

An activated FGFR3 clone containing the K650E mutation (FGFR3-TDII) was transfected into HEK293 cells. After an overnight starvation the receptor was immunoprecipitated from the cell lysate and subjected to *in vitro* kinase assays. In Figure 1A, γ-^{32}P-ATP was used in the kinase reactions after preincubating with NDGA for 15min. The NDGA concentration of 0.5 μM caused a dramatic reduction in the autophosphorylation of FGFR3-TDII. In Figures 1B and 1C the kinase reaction was performed in the absence of hot ATP and the phosphotyrosine on the receptor was detected by immunoblotting with a phospho-specific antibody. These results suggest a direct interaction of NDGA with FGFR3. To address if NDGA was inhibiting the ATP binding pocket of FGFR3-TDII, *in vitro* kinase reactions were performed over a range of ATP concentrations in the presence of the peptide substrate poly (4:1 Glu, Tyr). The incorporation of ^{32}P from [γ-^{32}P]-ATP into the peptide was quantified and plotted (Figure 1D). Increasing concentrations of ATP did not affect the K_m at various concentrations of NDGA, indicating the inhibitor NDGA is noncompetitive with ATP. Additionally, the inhibition of FGFR3-TDII autophosphorylation was independent of ATP over the same concentration range

(data not shown). This finding further supports the contention that NDGA is noncompetitive with ATP.

NDGA reduces in vivo autophosphorylation of FGFR3

To examine the *in vivo* effect of NDGA on the autophosphorylation of FGFR3-TDII and wild-type FGFR3, transfected HEK293 cells were treated with 40μM NDGA for 1 h. As seen in Figure 2A, the NDGA is able to reduce the autophosphorylation of both the wild-type and activated receptor. In Figure 2B the time dependence of the NDGA incubations was determined. A concentration of 30μM was able to begin to inhibit the receptor autophosphorylation in only 5 min and phosphorylation was almost completely gone by 60 min. Next we tested a broad range of NDGA concentrations with 40μM being the highest amount in order to examine the optimal effect. Figure 2C shows approximately 50% inhibition of FGFR3-TDII autophosphorylation with 10μM NDGA treatment. Also seen in Figure 2C, lower panel, there is a decrease in the amount of the immature form of the FGFR3-TDII receptor at 35μM NDGA. This is most likely due to the ability of NDGA to block ER/Golgi transport. Total cell lysate was examined for STAT1 activation in Figure 2D. The phosphorylation on Y701 of STAT1 caused by FGFR3-TDII is attenuated at the 20μM concentration of NDGA.

FGFR3 localization and Golgi breakdown with NDGA treatment

Typically, the disassembly of the Golgi begins to occur rapidily after only a few minutes of NDGA treatment and is reversible (23). As seen in Figure 3A, NDGA promoted the disassembly of the Golgi in approximately 15 min, while the subcellular localization of FGFR3-TDII appeared to become more punctate in the cytoplasm with increasing time. This may suggest that inhibition of the autophosphorylation of FGFR3-TDII by NDGA observed in Figure 2 is due to the change in the receptor localization and/or the altered interaction with downstream molecules. In order to examine this hypothesis, we expressed targeted kinase domains of activated FGFR3 (30) and treated the cells with NDGA for up to 1 h. As seen in Figure 3B, the myrR3-TDII derivative, which is targeted to the plasma membrane by a myristylation signal, exhibits membrane localization that is unaltered by NDGA treatment. Similarly, in Figure 3C the localization of the cytoR3-TDII derivative, targeted to the cytoplasm by a nonfunctional myristylation signal, appears unaltered with NDGA treatment.

NDGA reduction of FGFR3 downstream signaling

Next we examined the change in downstream signaling molecules that are activated in the FGFR3 pathway. Previous work from our lab has demonstrated the activation of STAT1, STAT3, and STAT5 in response to FGFR3 activation (31,32). Given the importance of STAT activation in a variety of human malignancies (33), we surveyed STAT1 and STAT3 for altered activation in response to NDGA treatment. The phosphorylation of MAPK was also determined. In Figure 4A, HEK293 transfected lysates were probed with phospho-specific antibodies for STAT1, STAT3 and MAPK. The signaling from FGFR3-TDII was greatly attenuated in response to NDGA. The low level of activation caused by the overexpression of FGFR3 wildtype was also inhibited by 30 μM NDGA in 5 min. As seen in Figure 4, there is an increase in phospho-MAPK at the 60 min time points. This is consistent with the previous report by Deshpande, which showed that the treatment of FL5.12 cells with NDGA led to an increase in activation of MAP kinases (34). In Figure 4B, as a control for the inhibition of autophosphorylation of FGFR3 by NDGA as seen above, FGFR3 was immunoprecipitated from the lysate and examined for phosphotyrosine. Next, in Figure 4C, we examined the STAT1 activation in HEK293 cells transfected with localized activated kinase domains of FGFR3. The phosphorylation on STAT1 caused by the expression of both myrR3-TDII and cytoR3-TDII was inhibited by 5 min of NDGA treatment. This would suggest that NDGA is able to block the signaling from an activated receptor independent of its localization. Curiously,

for unknown reasons, significantly enhanced STAT1 phosphorylation was observed in response to the cytoR3-TDII, even though expression of this FGFR3 derivative was previously shown to lack transforming activity (30).

Zilueton, a lipoxygenase inhbitor, does not block FGFR3-TDII autophosphorylation

In order to determine if the lipoxygenase (LOX) enzyme inhibiting activity of NDGA was important for its effect on FGFR signaling we examined another LOX inhibitor, Zileuton. Zileuton is a specific 5-LOX inhibitor while NDGA is non-specific (35,36). As seen in Figure 5A, when Zilueton was added to HEK293 cells transfected with FGFR3-TDII there was no decrease in receptor autohosphorylation. Even with 30 μM of Zilueton added for 1 h no change was detected. As a control, a duplicated plate was treated with 10 μM NDGA, which again shows a significant decrease in FGFR3-TDII autophosphorylation. This would imply that the ability of NDGA to inhibit lipoxygenase is not required to block FGFR signaling.

Overnight treatment with NDGA leads to increased apoptosis in FGFR3-TDII expressing cells

The above experiments were performed with very short term treatments of NDGA, less than 1 hr. Next we examined the effect of a 24 h exposure of various concentrations of NDGA on HEK293 FGFR3-TDII transfected cells. Poly (ADP-ribose) polymerase, PARP, is a zinc finger DNA-binding enzyme, which detects DNA strand breaks and is activated at an intermediate stage of apoptosis. During late stage apoptosis, PARP is cleaved and inactivated by the apoptotic proteases caspase-3 and caspase-7 (37). We examined the PARP cleavage in cell lysates treated with NDGA to determine the extent of apoptosis. As seen in Figure 5B, there is a significant increase in PARP cleavage in FGFR3-TDII-expressing cells as the concentration of NDGA is increased. Thus, in addition to the ability of NDGA to inhibit FGFR3 signaling, it is clearly able to increase cellular apoptosis.

NDGA increases apoptosis in a multiple myeloma cell line with activated FGFR3

To examine the possible therapeutic effects of NDGA for multiple myeloma, a lethal disease that is characterized by the slow proliferation of malignant plasma cells in the bone, we examined two multiple myeloma-derived cell lines that express high levels of mutated FGFR3 for an increase in apoptosis with NDGA treatment. As seen in Figure 5C, there is an increase in PARP cleavage in the KMS-18 cell line (FGFR3 G384D) with overnight treatment of NDGA. In Figure 5D, the same concentrations of NDGA did not seem to have a similar effect on the KMS-11 cell line (FGFR3 Y373C). This may indicate that NDGA is effective only on a subset of activating mutations in FGFR3, for example, kinase domain mutations but not extracellular domain mutations such as Y373C. Resolution of this question will require further detailed analysis.

NDGA blocks downstream signaling in multiple myeloma cells

First we examined the effect of NDGA on multiple myeloma cell lines treated with FGF2 to activate the FGFR3 receptor. The RPMI-8226 cell line contains “normal” levels of expression of wild-type FGFR3 while the LP-1 cell line has higher levels of FGFR3 expression. The cells were starved overnight and NDGA was added to the media for 1 h prior to stimulating the cells for 10 min by the addition of FGF2. As seen in Figure 6A, there is a significant decrease in MAPK activation with 30 μM NDGA treatment prior to stimulation, which would indicate that NDGA is able to inhibit the activation of endogenous, wildtype FGFR3. Next, we examined the effect of NDGA on MAPK activation in multiple myeloma cell lines that express high levels of mutationally activated FGFR3. As the concentration of NDGA increased with the 1 h treatment of the KMS-18 cell line, the phosphorylation on MAPK decreased in cell lysates (Figure 6B). These data suggest that NDGA is able to block signaling from FGFR3 that is activated by ligand or mutation. However, there was no significant change in MAPK activation

with the same concentrations of NDGA in the KMS-11 cell line as seen in Figure 6C, which may be dependent on the particular mutation of FGFR3; in the case of KMS-11, a Y373C mutation that introduces an abnormal disulfide bond in the extracellular domain.

Discussion

NDGA is a natural compound with an interesting history and broad spectrum of biological properties. Initially isolated from the creosote bush *Larrea divaricatta*, it was originally characterized as a potent antioxidant and shown to selectively inhibit arachidonic acid 5-lipoxygenase (38,39), thereby leading to a reduction of inflammatory pathways through decreased leukotriene and prostaglandin synthesis. NDGA also demonstrates profound effects on the secretory pathway, reflected in its ability to block protein transport from the ER to the Golgi apparatus, and to induce the redistribution of Golgi proteins into the ER (22–24,40). As a non-specific inhibitor of NADPH oxidase and protein kinase C, NDGA also disrupts the actin cytoskeleton and exerts effects on cell adhesion (41,42). Although some reports indicate that NDGA treatment can inhibit apoptosis, as in inhibition of CD95L-induced apoptosis of glioma cells (43), other reports demonstrate NDGA-induced apoptosis in a variety of cells, including human breast cancer cells, pancreatic carincoma cells, and HL-60 cells (44–46). NDGA has been shown to induce death receptor 5/TRAIL-R2 expression, thereby sensitizing malignant tumor cells to TRAIL-induced apoptosis (47). More recently, NDGA has been shown to directly inhibit activation of two RTKs, the insulin-like growth factor receptor (IGF-1R) and the c-erbB2/HER2/neu receptor, resulting in decreased cellular proliferation (25,27,48,49).

NDGA is a component of “Chaparral,” a natural product proposed several decades ago as a treatment for some cancers, but was removed from the FDA “generally recognized as safe” (GRAS) list in 1970. Since then, NDGA, also referred to as masoprocol, received FDA approval for inclusion in a topical cream Actinex, under FDA Application No. (NDA) 019940, for treatment of actinic keratoses. Recent studies of its properties have led to rekindled interest in its biochemical and chemotherapeutic properties, as evidenced by an ongoing clinical trial, “Phase I Study of NDGA in Patients With Nonmetastatic, Biochemically Relapsed Prostate Cancer on Androgen Dependent Prostate Cancer (ADPC)” (UCSF-035510) (48). Interestingly, different stereoisomers of NDGA occur, and whether these differ with regard to their biological properties has not been investigated. NDGA is found naturally as a mixture of chiral compounds, including the *meso* forms *R,R*-NDGA and *S,S*-NDGA, and the optically active form *S,R*-NDGA. In order to fully understand the spectrum of various biological activities exhibited by NDGA with regard to oncogenic RTKs such as IFG-1R and HER2 (25,27,49), or FGFR3 examined here, it may be desirable to synthesize chemically pure NDGA isomers for a thorough examination of their biological properties.

Given the importance of FGFR3 activation in several human cancers of clinical importance, it will be significant to determine whether the inhibitory properties of NDGA towards other RTKs, such as IGF-1R or HER2, apply to FGFR3. The activation of cellular signaling pathways by strongly activated mutants of FGFR3 such as the K650E mutant, responsible for Thanatophoric Dysplasia Type II (10), or the mutation K650M, responsible for Severe Achondroplasia with Delayed Development and Acanthosis Nigricans (SADDAN) (50), has been shown to occur within the secretory compartment, as evidenced by direct recruitment of Jak1 and STAT1 activation, and by Erk1/2 activation from the ER through FRS2α and PLCγ-independent pathways (18–20). Thus, the ability of NDGA to disrupt the secretory compartment, acting together noncompetitively with ATP and its previously demonstrated inhibitory properties towards others RTKs, suggests that it might be particularly effective against FGFR3.

Indeed, in the experiments described here, we demonstrate that NDGA exhibits strong inhibitory effects against FGFR3 kinase activity and the activation of downstream signaling pathways. Following expression in HEK293 cells and immunoprecipitation, the activated FGFR3 TDII mutant protein is directly inhibited when assayed for autophosphorylation activity. Furthermore, we demonstrate that although NDGA directly inhibits FGFR3-TDII kinase activity, it acts noncompetitively with ATP using this cell free assay. This mode of inhibition resembles that of a structurally similar compound, AG 538, which was shown to inhibit IGF-1R and act noncompetitively with ATP (51). This indicates NDGA may be a specific inhibitor toward FGFR3-TDII and other RTKs, rather than nonspecifically inhibiting a wide range of kinases. When cell lysates were examined for Tyr-phosphorylated FGFR3, a concentration of 30μM NDGA began to show inhibition of receptor phosphorylation in only 5 min, and receptor autophosphorylation was almost completely eliminated by 60 min. In this assay, the effects of NDGA were almost certainly the result of direct inhibition together with indirect inhibitory effects, such as disruption of protein secretion and collapse of the Golgi. This latter effect was clearly visible by immunofluorescent staining of the Golgi using the cis-Golgi marker 10E6. NDGA treatment also resulted in significantly diminished activation of STAT 1 and STAT3 by the FGFR3 TDII mutant. Prior work demonstrates that strongly activated mutants of FGFR3 actually recruit JAK1 directly to the ER leading to activation of STAT family members, which is not disrupted by brefeldin A (BFA) (18,19). In our results reported here, we found that NDGA, an agent previously shown to disrupt the Golgi by mechanisms distinct from BFA (52), rapidly blocked activation of STAT1 and STAT3. Although NDGA possesses strong antioxidant activity, the effects of NDGA on FGFR3 activation and signaling were not attributable solely to antioxidant activity, as shown by the inability of a chemically unrelated antioxidant, Zileuton, to affect FGFR3 activation. Using HEK293 cells expressing FGFR3, we demonstrated that NDGA significantly increases apoptosis for cells expressing the activated TDII mutant and in the multiple myeloma cell line KMS-18, as demonstrated by PARP cleavage. Lastly, using the multiple myeloma cell line LP-1 expressing FGFR3 WT, we show that FGF-dependent signaling, as reflected in the appearance of p-MAPK, is effectively blocked by NDGA treatment. NDGA also reduces p-MAPK in the KMS-18 multiple myeloma cell line expressing FGFR3 G384D.

Collectively, the results presented here indicate that NDGA, acting most likely by multiple mechanisms, including direct inhibition of kinase activity, disruption of the secretory pathway, inhibition of downstream signaling pathways, and increased apoptosis, possesses potentially beneficial attributes that merit further investigation. This is particularly true for those cancers where cellular proliferation depends upon continued stimulation of FGFR3 either by ligand activation or by mutational activation, as in bladder carcinoma and multiple myeloma.

Acknowledgments

We are grateful to Prof. Leslie Thompson of the University of California, Irvine (Irvine, CA) for providing us with human multiple myeloma cells, and Prof. Uli Muller for use of phosphorimaging equipment. We thank Kristy Drafahl and Lisa Salazar for technical assistance, and Laura Castrejon for editorial assistance. This work was supported by grants from the NIH (R01-CA90900) and from the Multiple Myeloma Research Foundation.

References

1. Manning G, Whyte DB, Martinez R, Hunter T, Sudarsanam S. The protein kinase complement of the human genome. Science 2002;298(5600):1912–34. [PubMed: 12471243]
2. Robertson SC, Tynan JA, Donoghue DJ. RTK mutations and human syndromeswhen good receptors turn bad. Trends Genet 2000;16(6):265–71. [PubMed: 10827454]
3. Jaye M, Schlessinger J, Dionne CA. Fibroblast growth factor receptor tyrosine kinases: molecular analysis and signal transduction. Biochim Biophys Acta 1992;1135(2):185–99. [PubMed: 1319744]

4. Johnson DE, Williams LT. Structural and functional diversity in the FGF receptor multigene family. Adv Cancer Res 1993;60:1–41. [PubMed: 8417497]
5. Bottcher RT, Niehrs C. Fibroblast growth factor signaling during early vertebrate development. Endocr Rev 2005;26(1):63–77. [PubMed: 15689573]
6. Ornitz DM. FGF signaling in the developing endochondral skeleton. Cytokine Growth Factor Rev 2005;16(2):205–13. [PubMed: 15863035]
7. Chen L, Deng CX. Roles of FGF signaling in skeletal development and human genetic diseases. Front Biosci 2005;10:1961–76. [PubMed: 15769677]
8. Dailey L, Ambrosetti D, Mansukhani A, Basilico C. Mechanisms underlying differential responses to FGF signaling. Cytokine Growth Factor Rev 2005;16(2):233–47. [PubMed: 15863038]
9. Wilkie AO, Morriss-Kay GM, Jones EY, Heath JK. Functions of fibroblast growth factors and their receptors. Curr Biol 1995;5(5):500–7. [PubMed: 7583099]
10. Tavormina PL, Shiang R, Thompson LM, et al. Thanatophoric dysplasia (types I and II) caused by distinct mutations in fibroblast growth factor receptor 3. Nat Genet 1995;9(3):321–8. [PubMed: 7773297]
11. Chesi M, Nardini E, Brents LA, et al. Frequent translocation t(4;14)(p16.3;q32.3) in multiple myeloma is associated with increased expression and activating mutations of fibroblast growth factor receptor 3. Nat Genet 1997;16(3):260–4. [PubMed: 9207791]
12. Richelda R, Ronchetti D, Baldini L, et al. A novel chromosomal translocation t(4; 14)(p16.3; q32) in multiple myeloma involves the fibroblast growth-factor receptor 3 gene. Blood 1997;90(10):4062–70. [PubMed: 9354676]
13. Sibley K, Stern P, Knowles MA. Frequency of fibroblast growth factor receptor 3 mutations in sporadic tumours. Oncogene 2001;20(32):4416–8. [PubMed: 11466624]
14. van Rhijn BW, Lurkin I, Radvanyi F, Kirkels WJ, van der Kwast TH, Zwarthoff EC. The fibroblast growth factor receptor 3 (FGFR3) mutation is a strong indicator of superficial bladder cancer with low recurrence rate. Cancer Res 2001;61(4):1265–8. [PubMed: 11245416]
15. Cappellen D, De Oliveira C, Ricol D, et al. Frequent activating mutations of FGFR3 in human bladder and cervix carcinomas. Nat Genet 1999;23(1):18–20. [PubMed: 10471491]
16. Rousseau F, el Ghouzzi V, Delezoide AL, et al. Missense FGFR3 mutations create cysteine residues in thanatophoric dwarfism type I (TD1). Hum Mol Genet 1996;5(4):509–12. [PubMed: 8845844]
17. Chesi M, Kuehl WM, Bergsagel PL. Recurrent immunoglobulin gene translocations identify distinct molecular subtypes of myeloma. Ann Oncol 2000;11 Suppl 1:131–5. [PubMed: 10707795]
18. Lievens PM, Liboi E. The thanatophoric dysplasia type II mutation hampers complete maturation of FGF receptor 3, which activates STAT1 from the endoplasmic reticulum. J Biol Chem. 2003
19. Lievens PM, Mutinelli C, Baynes D, Liboi E. The kinase activity of fibroblast growth factor receptor 3 with activation loop mutations affects receptor trafficking and signaling. J Biol Chem 2004;279 (41):43254–60. [PubMed: 15292251]
20. Lievens PM, Roncador A, Liboi E. K644E/M FGFR3 mutants activate Erk1/2 from the endoplasmic reticulum through FRS2 alpha and PLC gamma-independent pathways. J Mol Biol 2006;357(3):783–92. [PubMed: 16476447]
21. Fujiwara T, Misumi Y, Ikehara Y. Dynamic recycling of ERGIC53 between the endoplasmic reticulum and the Golgi complex is disrupted by nordihydroguaiaretic acid. Biochem Biophys Res Commun 1998;253(3):869–76. [PubMed: 9918822]
22. Fujiwara T, Misumi Y, Ikehara Y. Direct interaction of the Golgi membrane with the endoplasmic reticulum membrane caused by nordihydroguaiaretic acid. Biochem Biophys Res Commun 2003;301 (4):927–33. [PubMed: 12589801]
23. Fujiwara T, Takami N, Misumi Y, Ikehara Y. Nordihydroguaiaretic acid blocks protein transport in the secretory pathway causing redistribution of Golgi proteins into the endoplasmic reticulum. J Biol Chem 1998;273(5):3068–75. [PubMed: 9446623]
24. Drecktrah D, de Figueiredo P, Mason RM, Brown WJ. Retrograde trafficking of both Golgi complex and TGN markers to the ER induced by nordihydroguaiaretic acid and cyclofenil diphenol. J Cell Sci 1998;111 (Pt 7):951–65. [PubMed: 9490639]

25. Blecha JE, Anderson MO, Chow JM, et al. Inhibition of IGF-1R and lipoxygenase by nordihydroguaiaretic acid (NDGA) analogs. Bioorg Med Chem Lett 2007;17(14):4026–9. [PubMed: 17502145]
26. Meyer GE, Chesler L, Liu D, et al. Nordihydroguaiaretic acid inhibits insulin-like growth factor signaling, growth, and survival in human neuroblastoma cells. J Cell Biochem 2007;102:1529–41. [PubMed: 17486636]
27. Youngren JF, Gable K, Penaranda C, et al. Nordihydroguaiaretic acid (NDGA) inhibits the IGF-1 and c-erbB2/HER2/neu receptors and suppresses growth in breast cancer cells. Breast Cancer Res Treat 2005;94(1):37–46. [PubMed: 16142439]
28. Domin J, Higgins T, Rozengurt E. Preferential inhibition of platelet-derived growth factor-stimulated DNA synthesis and protein tyrosine phosphorylation by nordihydroguaiaretic acid. J Biol Chem 1994;269(11):8260–7. [PubMed: 7510683]
29. Webster MK, D'Avis PY, Robertson SC, Donoghue DJ. Profound ligand-independent kinase activation of fibroblast growth factor receptor 3 by the activation loop mutation responsible for a lethal skeletal dysplasia, thanatophoric dysplasia type II. Mol Cell Biol 1996;16(8):4081–7. [PubMed: 8754806]
30. Webster MK, Donoghue DJ. Enhanced signaling and morphological transformation by a membrane-localized derivative of the fibroblast growth factor receptor 3 kinase domain. Mol Cell Biol 1997;17 (10):5739–47. [PubMed: 9315632]
31. Hart KC, Robertson SC, Donoghue DJ. Identification of tyrosine residues in constitutively activated fibroblast growth factor receptor 3 involved in mitogenesis, Stat activation, and phosphatidylinositol 3-kinase activation. Mol Biol Cell 2001;12(4):931–42. [PubMed: 11294897]
32. Hart KC, Robertson SC, Kanemitsu MY, Meyer AN, Tynan JA, Donoghue DJ. Transformation and Stat activation by derivatives of FGFR1, FGFR3, and FGFR4. Oncogene 2000;19(29):3309–20. [PubMed: 10918587]
33. Buettner R, Mora LB, Jove R. Activated STAT signaling in human tumors provides novel molecular targets for therapeutic intervention. Clin Cancer Res 2002;8(4):945–54. [PubMed: 11948098]
34. Deshpande VS, Kehrer JP. Oxidative stress-driven mechanisms of nordihydroguaiaretic acid-induced apoptosis in FL5.12 cells. Toxicol Appl Pharmacol 2006;214(3):230–6. [PubMed: 16473382]
35. Carter GW, Young PR, Albert DH, et al. 5-lipoxygenase inhibitory activity of zileuton. J Pharmacol Exp Ther 1991;256(3):929–37. [PubMed: 1848634]
36. Tang DG, Chen YQ, Honn KV. Arachidonate lipoxygenases as essential regulators of cell survival and apoptosis. Proc Natl Acad Sci USA 1996;93(11):5241–6. [PubMed: 8643560]
37. Decker P, Muller S. Modulating poly (ADP-ribose) polymerase activity: potential for the prevention and therapy of pathogenic situations involving DNA damage and oxidative stress. Curr Pharm Biotechnol 2002;3(3):275–83. [PubMed: 12164482]
38. Salari H, Braquet P, Borgeat P. Comparative effects of indomethacin, acetylenic acids, 15-HETE, nordihydroguaiaretic acid and BW755C on the metabolism of arachidonic acid in human leukocytes and platelets. Prostaglandins Leukot Med 1984;13(1):53–60. [PubMed: 6424136]
39. Chang J, Skowronek MD, Cherney ML, Lewis AJ. Differential effects of putative lipoxygenase inhibitors on arachidonic acid metabolism in cell-free and intact cell preparations. Inflammation 1984;8(2):143–55. [PubMed: 6430801]
40. Tagaya M, Henomatsu N, Yoshimori T, Yamamoto A, Tashiro Y, Mizushima S. Inhibition of vesicle-mediated protein transport by nordihydroguaiaretic acid. J Biochem 1996;119(5):863–9. [PubMed: 8797085]
41. Holland JA, Goss RA, O'Donnell RW, Chang MM, Johnson DK, Ziegler LM. Low-density lipoprotein induced actin cytoskeleton reorganization in endothelial cells: mechanisms of action. Endothelium 2001;8(2):117–35. [PubMed: 11577705]
42. Papadogiannakis N, Barbieri B. Lipoxygenase inhibitors counteract protein kinase C mediated events in human T lymphocyte proliferation. Int J Immunopharmacol 1997;19(5):263–75. [PubMed: 9439765]
43. Wagenknecht B, Schulz JB, Gulbins E, Weller M. Crm-A, bcl-2 and NDGA inhibit CD95L-induced apoptosis of malignant glioma cells at the level of caspase 8 processing. Cell Death Differ 1998;5 (10):894–900. [PubMed: 10203695]

44. Park S, Hahm ER, Lee DK, Yang CH. Inhibition of AP-1 transcription activator induces myc-dependent apoptosis in HL60 cells. J Cell Biochem 2004;91(5):973–86. [PubMed: 15034932]
45. Nishimura K, Tsumagari H, Morioka A, et al. Regulation of apoptosis through arachidonate cascade in mammalian cells. Appl Biochem Biotechnol 2002;102–103(1–6):239–50.
46. Tong WG, Ding XZ, Adrian TE. The mechanisms of lipoxygenase inhibitor-induced apoptosis in human breast cancer cells. Biochem Biophys Res Commun 2002;296(4):942–8. [PubMed: 12200139]
47. Yoshida T, Shiraishi T, Horinaka M, et al. Lipoxygenase inhibitors induce death receptor 5/TRAIL-R2 expression and sensitize malignant tumor cells to TRAIL-induced apoptosis. Cancer Sci 2007;98 (9):1417–23. [PubMed: 17645780]
48. Ryan CJ, Harzstark AH, Rosenberg J, et al. A pilot dose-escalation study of the effects of nordihydroguareacetic acid on hormone and prostate specific antigen levels in patients with relapsed prostate cancer. BJU Int 2008;101(4):436–9. [PubMed: 18234062]
49. Zavodovskaya M, Campbell MJ, Maddux BA, et al. Nordihydroguaiaretic acid (NDGA), an inhibitor of the HER2 and IGF-1 receptor tyrosine kinases, blocks the growth of HER2-overexpressing human breast cancer cells. J Cell Biochem 2007;103:624–35. [PubMed: 17562544]
50. Tavormina PL, Bellus GA, Webster MK, et al. A novel skeletal dysplasia with developmental delay and acanthosis nigricans is caused by a Lys650Met mutation in the fibroblast growth factor receptor 3 gene. Am J Hum Genet 1999;64(3):722–31. [PubMed: 10053006]
51. Blum G, Gazit A, Levitzki A. Substrate competitive inhibitors of IGF-1 receptor kinase. Biochemistry 2000;39(51):15705–12. [PubMed: 11123895]
52. Kim SM, Park TW, Park JW. Effect of nordihydroguaiaretic acid on the secretion of lipoprotein lipase. J Biochem Mol Biol 2002;35(5):518–23. [PubMed: 12359096]

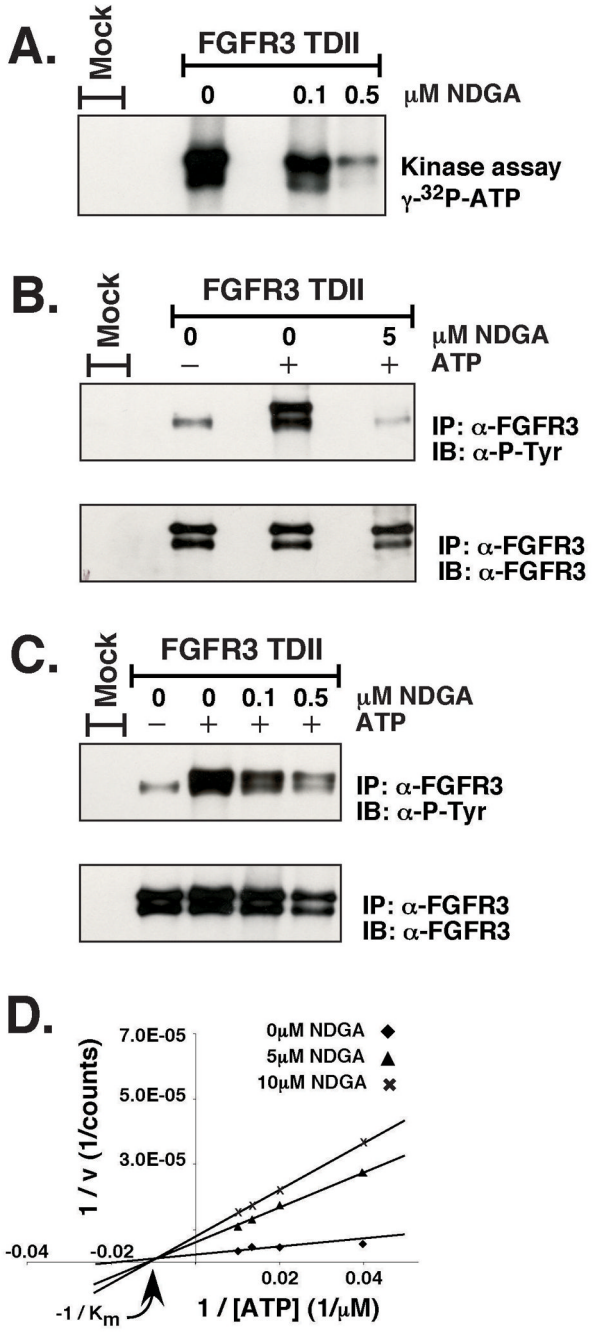

Figure 1. In vitro kinase assays

FGFR3-TDII was transfected into HEK293 cells. 24 h after transfection, cells were starved overnight in media containing no serum. Cells were collected and lysed in 1% NP-40 Lysis Buffer. FGFR3-TDII was immunoprecipitated from lysates as described in Experimental Procedures. Immunoprecipitates were preincubated with 0.1μM, 0.5μM, or 5μM NDGA in Kinase Buffer for 15 min on ice before the addition of ATP and incubation at 37°C for 15 min. Proteins were separated by 7.5% SDS-PAGE. The kinase reactions in **(A)** were performed with 5μCi [γ-^{32}P]-ATP per sample. The gel was dried and exposed to film directly. The kinase reactions in **(B)** and **(C)** were performed with 150μM ATP. The gels were transferred to Immobilon-P membranes for immunoblotting with anti-phosphotyrosine (4G10) antisera

(top). The membranes were stripped and reprobed with FGFR3 antiserum **(bottom)**. Antibodies were detected by ECL. **(D)** Kinase reactions were performed using FGFR3-TDII immunoprecipitates obtained as in **(A)**, with 80 μg/mL of the poly (4:1 Glu, Tyr) (Sigma) peptide substrate and increasing amounts of ATP (25 μM, 50 μM, 75 μM, 100 μM) under increasing NDGA concentrations (0 μM, 5 μM, 10 μM). The reactions were separated by 10% SDS PAGE. After staining, destaining, and drying, the gel was visualized using a Phosphorimager (Bio-Rad). Quantification of radioactive bands was performed using the Quantity One software (Bio-Rad).

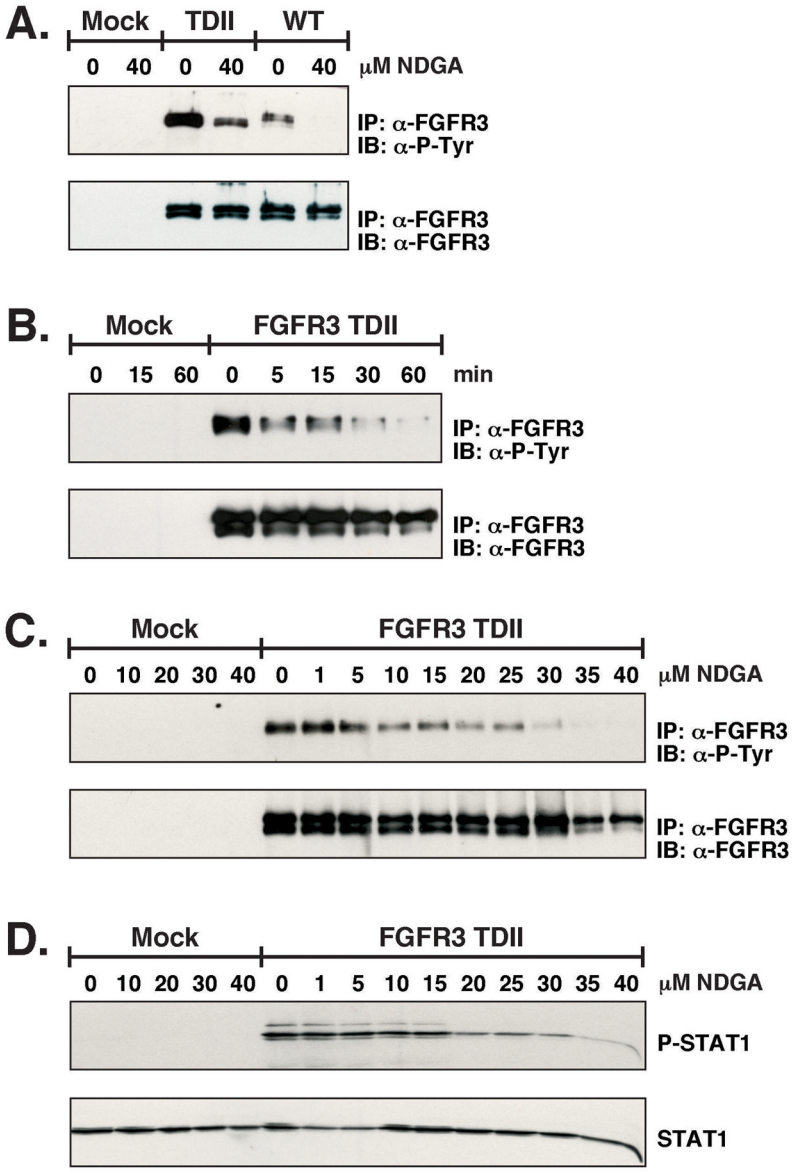

Figure 2. In vivo autophosphorylation of FGFR3

HEK293 transfected cells were starved overnight prior to treatment with NDGA. Cells were collected and lysed in 1% NP-40 Lysis Buffer. In **(A)** FGFR3-TDII and FGFR3-WT expressing cells were treated with 40μM NDGA for 1 h. FGFR3 was immunoprecipitated from lysates, separated by 10% SDS-PAGE, and transferred to Immobilon-P membrane for immunoblotting with anti-phosphotyrosine (4G10) **(top)** and FGFR3 antisera **(bottom)**. Antibodies were detected by ECL. In **(B)** FGFR3-TDII expressing cells were treated with 30μM NDGA. Cells were collected and lysed at the indicated times. Immunoprecipitations and immunuoblotting was performed as in **(A)**. In **(C)** FGFR3-TDII expressing cells were treated with a range of NDGA (0, 1, 5, 10, 15, 20, 25, 30, 35 and 40μM) for 1 h prior to collecting in 1% NP-40 Lysis Buffer. FGFR3-TDII was immunoprecipitated and immunoblotted as in **(A)**. In **(D)** 35μg of total cell lysate from **(C)** was separated by 10% SDS-PAGE and transferred to Immobilon-P membrane. The membrane was first immunoblotted with anti-Phospho-STAT1 and then stripped and reprobed for total STAT1.

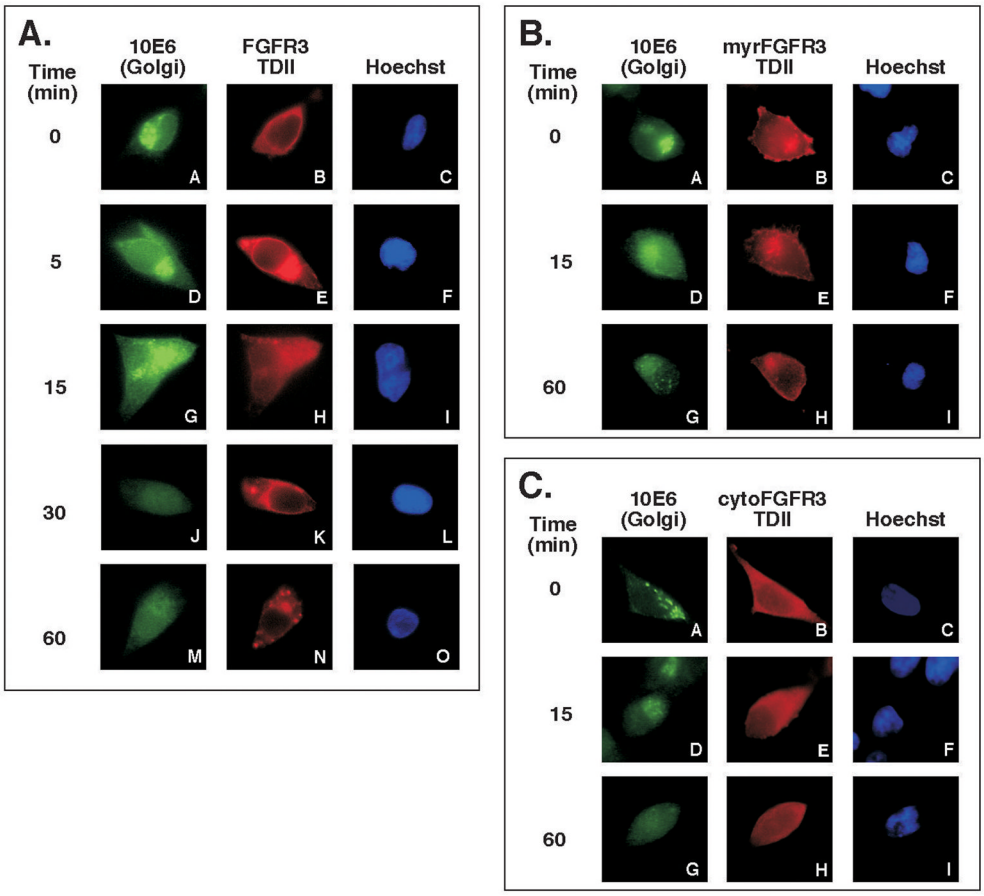

Figure 3. FGFR3-TDII localization with NDGA treatment

HEK293 cells were plated on 10cm dishes containing Collagen type I coated glass coverslips one day prior to transfecting with **(A)** FGFR3-TDII, **(B)** myrR3-TDII or **(C)** cytoR3-TDII. 24 h after transfection, cells were starved overnight in media containing no serum. NDGA was diluted in DMSO and added to the plates at a final concentration of 30μM. Coverslips were fixed with 3% paraformaldehyde/PBS at the indicated times. The 0 time point was treated with DMSO. The cis-Golgi was detected with monoclonal AB 10E6 and fluorescein-conjugated anti mouse secondary antibody. FGFR3 localization was detected with rabbit polyclonal antibody FGFR3(C-15) and rhodamine-conjugated anti rabbit secondary antibody. The nuclei were visualized by Hoechst dye added to the Rh secondary antibody mix.

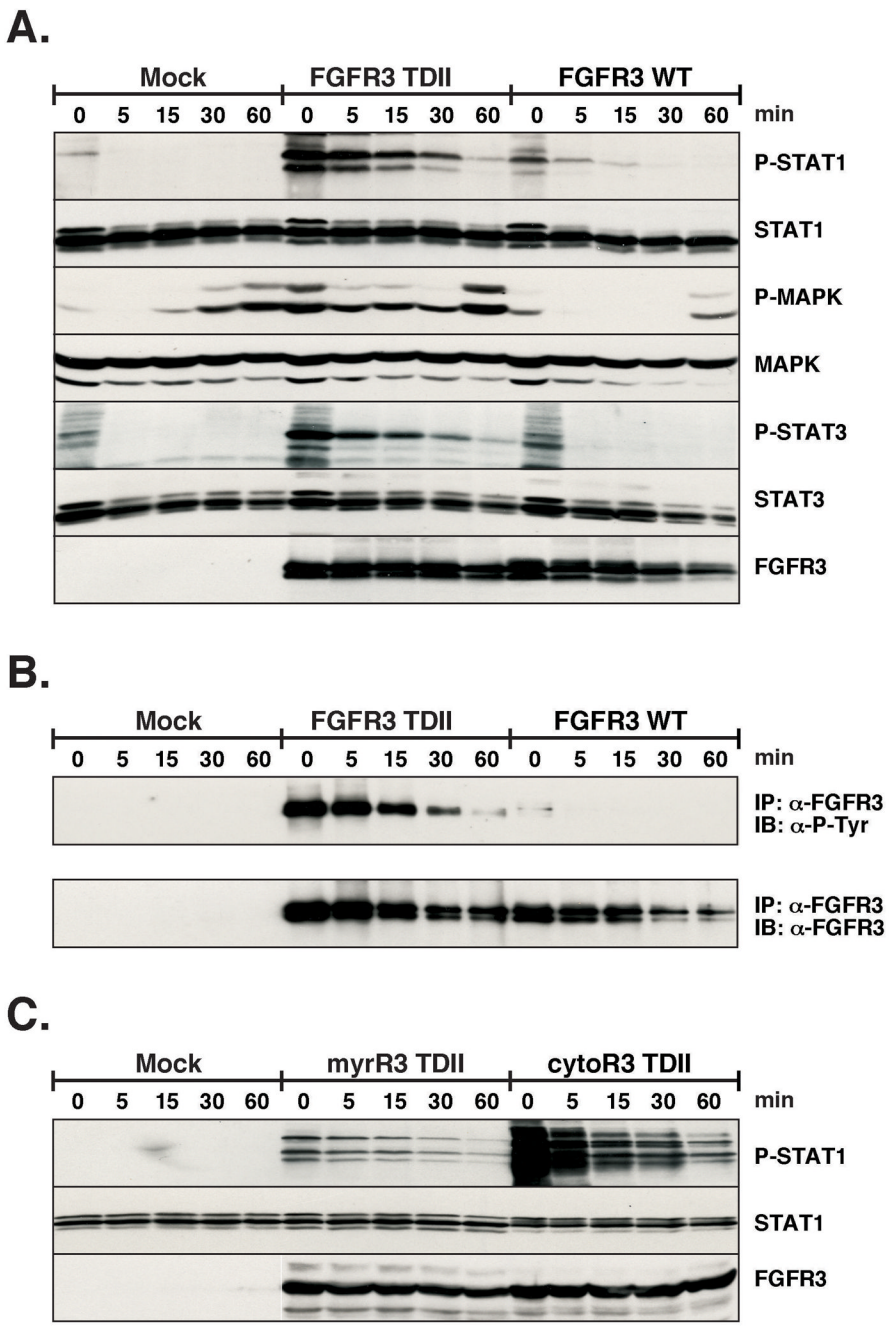

Figure 4. Alteration of FGFR3 signaling

HEK293 cells were transfected with FGFR3-TDII and WT. 24 h after transfection, cells were starved overnight. Plates were treated with 30μM NDGA for the indicated times. Cells were collected and lysed in RIPA Lysis Buffer. **(A)** Duplicate sets of 40μg of lysate were separated by 10% SDS-PAGE, transferred to Immobilon-P membrane and immunoblotted. The first membrane was cut in half horizontally and the top was probed with phospho-STAT1, STAT1 and FGFR3 antisera, sequentially. The bottom was immunoblotted with phospho-MAPK and MAPK. The second membrane was immunoblotted with phosph-STAT3 and STAT3 antisera. Membranes were stripped of bound antibodies between primary incubations. **(B)** 200μg of lysate was immunoprecipitaed with FGFR3 antiserum. Proteins were separated by 10% SDS-

PAGE, and transferred to Immobilon-P membrane for immmunoblotting with anti-phosphotyrosine (4G10) **(top)** and FGFR3 antisera **(bottom)**. Antibodies were detected by ECL. **(C)** HEK293 cells were transfected with myrR3-TDII and cytoR3-TDII. 24 h after transfection, cells were starved overnight. Plates were treated with 30μM NDGA for the indicated times. Cells were collected and lysed in RIPA Lysis Buffer. 30μg of lysate were separated by 10% SDS-PAGE, transferred to Immobilon-P membrane and immunoblotted. The membrane was cut in half horizontally and the top was probed with phospho-STAT1 and STAT1 antisera, sequentially. The bottom was immunoblotted with FGFR3 antisera.

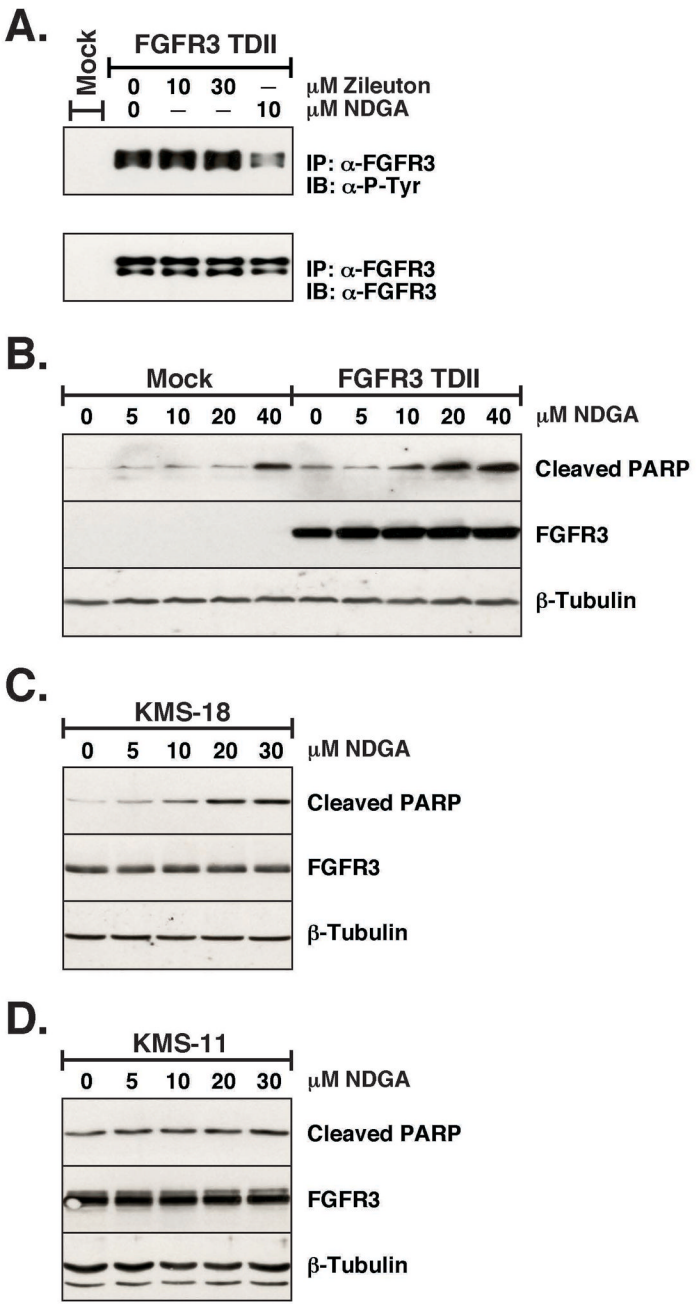

Figure 5. Induction of apoptosis by NDGA, and comparison with Zilueton, another lipoxygenase inhbitor

(A) HEK293 transfected cells were starved overnight prior to treatment with Zilueton or NDGA. Cells were collected and lysed in 1% NP-40 Lysis Buffer. FGFR3-TDII was immunoprecipitated from 250μg of lysate, separated by 10% SDS-PAGE, and transferred to Immobilon-P membrane for immmunoblotting with anti-phosphotyrosine (4G10) **(top)** and FGFR3 antisera **(bottom)**. Antibodies were detected by ECL. The membrane was stripped between each antibody incubation. **(B)** Apoptosis was assayed by PARP cleavage in HEK293 cells transfected with FGFR3-TDII or pcDNA3 (mock), treated for 24 h with a concentration range of NDGA in 10% FBS media. Cells were collected and lysed in 1% NP-40 Lysis Buffer. 30μg of lysate was separated by 15% SDS-PAGE, transferred to Immobilon-P membrane and

immunoblotted with **(top)** cleaved PARP (Asp214), **(middle)** FGFR3 and **(bottom)** beta-tubulin antisera, followed by ECL. The membrane was stripped between each antibody incubation. KMS-18 **(C)** or KMS-11 **(D)** cells were treated for 24 h with 0, 5, 10, 20 or 30μM NDGA. 30μg of lysate was separated by 10% SDS-PAGE, transferred to Immobilon-P membrane and immunoblotted as in **(B)**.

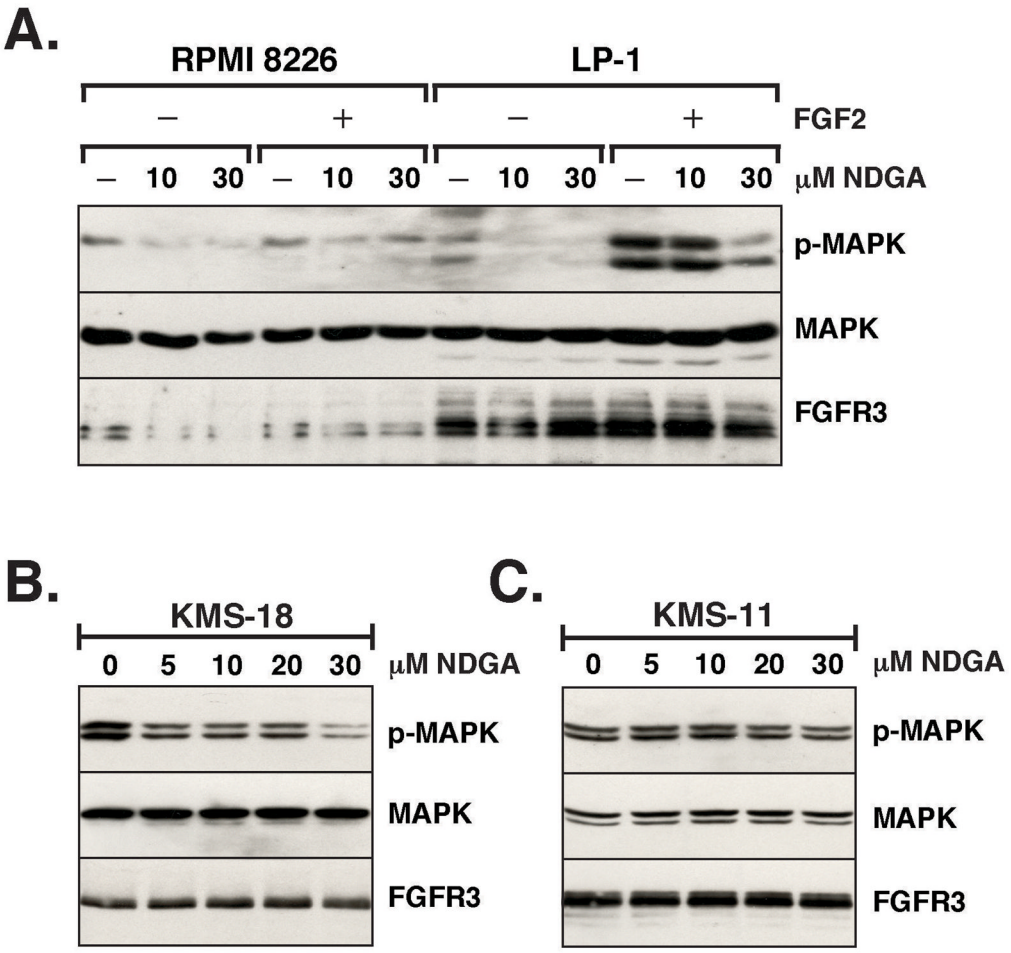

Figure 6. Downstream effect of NDGA on Multiple Myeloma cells

(A) The Multiple Myeloma cell lines RPMI 8226 and LP-1 were starved overnight in RPMI 1640 media with 0% serum in 6 well dishes. Duplicate wells for each cell type were preincubated with 0, 10 or 30μM NDGA for 1 h. Half the cells were then treated with 10ng/ml FGF2 and 1μg/ml Heparin for 10 min. Cells were collected and lysed in RIPA Lysis Buffer. 30 μg of lysate was separated by 10% SDS-PAGE, transferred to Immobilon-P membrane and immunoblotted with **(top)** phospho-p44/42 MAPK, **(middle)** MAP Kinase (ERK1 + ERK2) and **(bottom)** FGFR3 antisera, followed by ECL. The membrane was stripped between each antibody incubation. KMS-18 cells **(B)** or KMS-11 cells **(C)** cells were treated for 1 h with 0, 5, 10, 20 or 30μM NDGA. Cells were collected, treated and immunoblotted as in **(A)**.